water

Article

CSM-CERES-Wheat Sensitivity to Evapotranspiration Modeling Frameworks under a Range of Wind Speeds

Milad Nouri [1,*], Gerrit Hoogenboom [2], Mohammad Bannayan [3] and Mehdi Homaee [4,5]

1 Soil and Water Research Institute, Agricultural Research, Education and Extension Organization (AREEO), Karaj P.O. Box 31779-93545, Iran
2 Department of Agricultural and Biological Engineering, University of Florida, Gainesville, FL 32611-0570, USA
3 Department of Agronomy, Ferdowsi University of Mashhad, Mashhad P.O. Box 91775-1163, Iran
4 Department of Mining and Environmental Engineering, Faculty of Engineering, Tarbiat Modares Univesity, Tehran 14115, Iran
5 Agrohydrology Research Group, Tarbiat Modares University, Tehran 14115, Iran
* Correspondence: m.nouri@modares.ac.ir

Abstract: Crop modeling uncertainty is expected to be high under weather data limitations; thus, jeopardizing decision-making on food-water security. Missing near-surface wind speed (u_2) data required to accurately estimate reference evapotranspiration (ET_o) seemed to significantly affect both the potential evapotranspiration (ET_P) and yield simulations for data-scarce windy regions. In this study, the uncertainty in crop modeling based on different ET_P approaches was assessed. In this regard, wheat yield and evapotranspiration were simulated with the CSM-CERES-Wheat model using either the Priestley-Taylor/Ritchie (PT) or the Penman-Monteith DSSAT (PM) methods under "rain-fed, low-nitrogen stress", "rain-fed, high nitrogen stress", "full irrigation, low nitrogen stress", and "full irrigation, high nitrogen stress" scenarios for a u_2 range from 0.8 to 3.5 m s^{-1}. The daily weather data required to run the model were retrieved from 18 semi-arid areas located in western Iran. The statistically significant differences in mean yield and cumulative distribution were determined by the non-parametric Wilcoxon signed-rank and the Kolmogorov-Smirnov tests, respectively. The deviation in evaporation and transpiration simulated by applying PT and PM was lower under rain-fed condition. Under "rain-fed, low-nitrogen stress", the PT-simulated yield deviated significantly ($p < 0.05$) from PM-simulated yield by more than 26% for the sites with u_2 above 3 m s^{-1}. The deviation in ET_P estimates did not, however, lead to statistically significant difference in yield distribution curves for almost all sites and scenarios. Nitrogen deficiency resulted in a smaller difference in yield for rain-fed condition. The yield results showed a deviation below 6% under full irrigation condition. Under windy rain-fed condition, high deviation in leaf area index (LAI) and ET_P estimates caused a large difference in the actual transpiration to potential transpiration ratio (T_a/T_P), and yield. However, the deviation between PT- and PM-simulated LAI and T_a/T_P for the full irrigation scenarios was less than 6%. Overall, the results from this study indicate that when soil moisture is depleted, resembling rain-fed condition, simulation of yield appears to be highly sensitive to the estimation of ET_P for windy areas.

Keywords: crop modeling; data limitation; water-nitrogen stress; water-limited regions

check for updates

Citation: Nouri, M.; Hoogenboom, G.; Bannayan, M.; Homaee, M. CSM-CERES-Wheat Sensitivity to Evapotranspiration Modeling Frameworks under a Range of Wind Speeds. *Water* **2022**, *14*, 3023. https://doi.org/10.3390/w14193023

Academic Editor: Luis Santos Pereira

Received: 18 July 2022
Accepted: 19 September 2022
Published: 26 September 2022

1. Introduction

Water availability is among the most limiting factor for crop production and must be well managed, particularly for water-limited regions. Population growth, water governance gaps, a low productivity, and climate change cause consumptive water use to exceed water supply replenishment, a phenomenon known as water scarcity [1,2]. Since more than 90% of water consumption is dedicated to the agricultural sector in water-stressed areas, proper agricultural water management is crucial in these regions [2,3].

Crop models are important components of decision support systems (DSS) for food-water security [4–6]. Due to improvements in computational technology, a number of sophisticated crop models have been developed to simulate crop growth, development, and yield, as well as crop response to environmental changes and stresses [5,6]. Although most crop models are accessible and easy-to-use, uncertainties surrounding the results may jeopardize the policymaking processes [7,8]. Model structure, model inputs, and model parameters are three sources of uncertainty in simulations that have been generally addressed in the literature [7–10]. Uncertainties in model structure are associated with mathematical equations used in the models. Input uncertainty arises from the incorrect climatic (e.g., wind speed), pedologic (e.g., soil texture), and hydrologic (e.g., soil saturated hydraulic conductivity) measurements required to run crop models [11–13]. Parameters (e.g., light extinction coefficient used for evapotranspiration partitioning) are model components which cannot be directly measured, but often obtained by calibration based on reliable data sets, and any error in estimating parameters and coefficients adds uncertainty to the outputs [7–10].

Evapotranspiration is of great significance in crop modeling as it is a key component of the water balance and thus, affects processes such as soil water dynamics and, ultimately, final yield [14,15]. Since an accurate measurement of the crop evapotranspiration is a tool-demanding and complex task, it is often estimated using the two-step approach which bases on the estimation of the reference evapotranspiration (ET_o) [16–18]. The ET_o is the evapotranspiration rate of a theoretical crop having an assumed height of 12 cm, a fixed surface resistance of 70 s m^{-1}, and an albedo of 0.23, closely resembling evapotranspiration from an extensive green grass surface with uniform height, actively growing, well-watered, and completely shading the ground [19]. Multiplying ET_o by the crop coefficients (K_c), crop evapotranspiration can be estimated in absence of environmental and water stresses (i.e., standard condition) [18,19]. The crop evapotranspiration under standard condition can be considered as potential evapotranspiration (ET_P) [19,20]. All three above-mentioned types of uncertainties can be found for evapotranspiration estimation [14,21]. The parameter-related uncertainties in evapotranspiration estimation are mainly linked to factors such as extinction parameter (K_{ext}, applied for evapotranspiration partitioning) or crop coefficient (K_c) considered for a specific crop. There are uncertainties associated with the parameters of evapotranspiration modeling. Sau, et al. [22] and López-Cedrón, et al. [23], therefore, suggested that the performance of crop models can be improved by reducing the default extinction partitioning factor. However, they mentioned that changing the default K_c is unlikely to be promising for crop modeling. Input uncertainties in estimating ET_o, and consequently actual evapotranspiration, are generated when the required data, such as relative humidity, vapor pressure deficit, dew point temperature, wind speed or solar radiation, are lacking or are of questionable quality [24–26]. Thorp, et al. [14] indicated that more input-demanding ET_o equations such as Penman-Monteith DSSAT (PM) [19] and standardized ASCE Penman-Monteith (ASCE-PM) [27] are more reliable with respect to the less input-demanding ET_P models such as Priestley-Taylor/Ritchie equation (PT) [28] for crop modeling. However, users have to utilize less-input demanding models when the required weather data are partially missing. Hence, an input limitation is likely to lead to model structure-related uncertainties. In other words, when a specific weather variable, for instance wind speed data, is missing or of poor quality, modelers employ ET_o alternatives that do not require this weather variable as an input or use the approaches suggested in the literature, such as those proposed by Allen, et al. [19] or Hargreaves and Samani [29], to approximate the missing records.

Several studies in climatology and hydrology have addressed the role of missing data or data quality in ET_o simulations [24,30–33]. These studies have primarily considered PM proposed by Allen, et al. [19] as the benchmark for evaluating other equations. PM has been recommended by the Food and Agricultural Organization of the United Nations (FAO) and the International Commission for Irrigation and Drainage (ICID) as a standard method for reference evapotranspiration estimation [34]. This model has also been suggested for soil-crop modeling if all required data, i.e., minimum and maximum temperature, wind speed, solar radiation and relative humidity or dew point temperature, are available [14,22,23,35,36]. The application of other options to calculate ET_o when data are lacking has been also suggested [28,29,37,38]. However, the condition for which an alternative formula such as PT can be applied for robust crop modeling using incomplete sets of data has not been explicitly discussed. Near-surface wind speed is one of the most important inputs required for calculating ET_o by PM, particularly in water-limited arid and semi-arid regions, where it has been found to be the major contributing variable affecting ET_o dynamics [39–44]. Consequently, application of alternatives that do not consider wind speed may lead to highly uncertain modeling results in wind-affected, water-limited environments [45,46]. Stresses, e.g., water shortage and nitrogen deficiency, affect yield through reducing the evapotranspiration rate [47,48]. Such stresses influence the yield response to evapotranspiration rate, and consequently, the accuracy of yield modeling. Additionally, the effects of a specific stress (e.g., drought) on evapotranspiration may be modulated by other stresses. This is why the data-driven models associating yield loss to crop evapotranspiration deficit based on a response factor are valid for the conditions under which other inputs, such as nitrogen, are sufficiently supplied [49]. Process-based crop models can simulate the coupled stresses effects; thus, they are more suited to be applied for assessing the sensitivity of crop models to estimates of evapotranspiration. Including the coupled effects of stresses, such as nitrogen deficit, provides insights into our understanding of crop modeling sensitivity to evapotranspiration approaches under data scarcity. The objective of this study was, therefore, to determine the deviation in wheat yield simulated by CSM-CERES-Wheat using Penman-Monteith DSSAT (PM) and Priestley-Taylor/Ritchie (PT) evapotranspiration approaches for different water and nitrogen stress scenarios across a broad range of wind speeds.

2. Materials and Methods

2.1. Study Area and Data Sets

The analyses were conducted for 18 water-limited semi-arid areas in the western half of Iran with aridity indices (AI), defined as the annual ratio of precipitation to PM-estimated ET_o according to UNEP [50], ranging from 0.20 to 0.37 (Figure 1). These regions are considered as water-limited environments experiencing an increasing trend in meteorological droughts during the recent half-century [51,52]. Cultivating wheat under rain-fed and irrigated conditions is common in the study area [53]. The range of minimum temperature, maximum temperature and precipitation for the average duration of the growing season is −1.5–4.3 °C, 11.4–17.1 °C, and 170–382 mm, respectively (Table 1). The surveyed sites cover a wide range of wind speeds at a height of 2 m (u_2), i.e., from 0.78 to 3.47 m s^{-1} during the winter wheat growing season (Table 1). Wind speed greatly contributes to the ET_P dynamics in these regions and, therefore, a reliable estimation of ET_P is likely to be highly dependent on the availability of wind speed data.

Table 1. Geographic and climatic characteristics of the study sites.

No.	Station	Longitude	Latitude	Elevation	AI $^{\beta}$	u_2 *	P *	Tmin *	Tmax *
		(°E)	(°N)	m.a.s.l $^{\alpha}$	-	m s^{-1}	mm	°C	
1	Ahar	47°04′	38°26′	1390	0.24	2.45	206	1.4	12.7
2	Aligodarz	49°42′	33°24′	2022	0.25	3.21	342	1.2	13.5
3	Arak	49°46′	34°06′	1708	0.21	1.35	238	1.7	13.7
4	Ardebil	48°17′	38°15′	1332	0.29	3.02	201	0.2	12.3
5	Bijar	47°37′	35°53′	1883	0.21	3.12	251	1.6	11.5
6	Borojerd	48° 45′	33°55′′	1629	0.28	2.65	382	2.6	14.1
7	Hamedan	48°32′	34°52′	1741	0.23	1.69	242	0.2	13.7
8	Kermanshah	47°09′	34°21′	1318	0.26	1.89	325	1.8	15.6
9	Khorramabad	48°17′	33°26′	1148	0.29	1.63	373	2.9	16.4
10	Khoy	44° 58′	38°33′	1103	0.24	1.29	205	1.7	13.2

Table 1. *Cont.*

No.	Station	Longitude	Latitude	Elevation	AI $^{\beta}$	u_2 *	P *	Tmin *	Tmax *
		(°E)	(°N)	m.a.s.l $^{\alpha}$	-	m s^{-1}	mm	°C	
11	Nozheh	48°43′	35°12′	1680	0.23	2.10	254	−1.5	12.7
12	Qorveh	47°48′	35°10′	1906	0.23	2.21	262	1.4	12.1
13	Saghez	46°16′	36°15′	1523	0.32	1.92	318	−1.2	13.0
14	Sahand	46°07′	37°56′	1641	0.20	3.47	170	3.2	11.4
15	Shemiran	51°29′	35°48′	1549	0.37	0.78	335	4.3	13.7
16	Urmia	45°03′	37°40′	1328	0.24	1.73	222	1.2	13.1
17	Zanjan	48°29′	36°41′	1663	0.22	2.01	232	0.7	13.2
18	Zarghan	52°43′	29°47′	1596	0.21	1.05	274	2.0	17.1

Notes: $^{\alpha}$ The "m.a.s.l" refers to meters above sea level. $^{\beta}$ AI indicates the annual aridity index. * The average values of near-surface wind speed (u_2), precipitation (P), minimum (Tmin) and maximum (Tmax) temperature during the growing season for the four scenarios that were used in this study. The weather data are based on the period of 1996–2016.

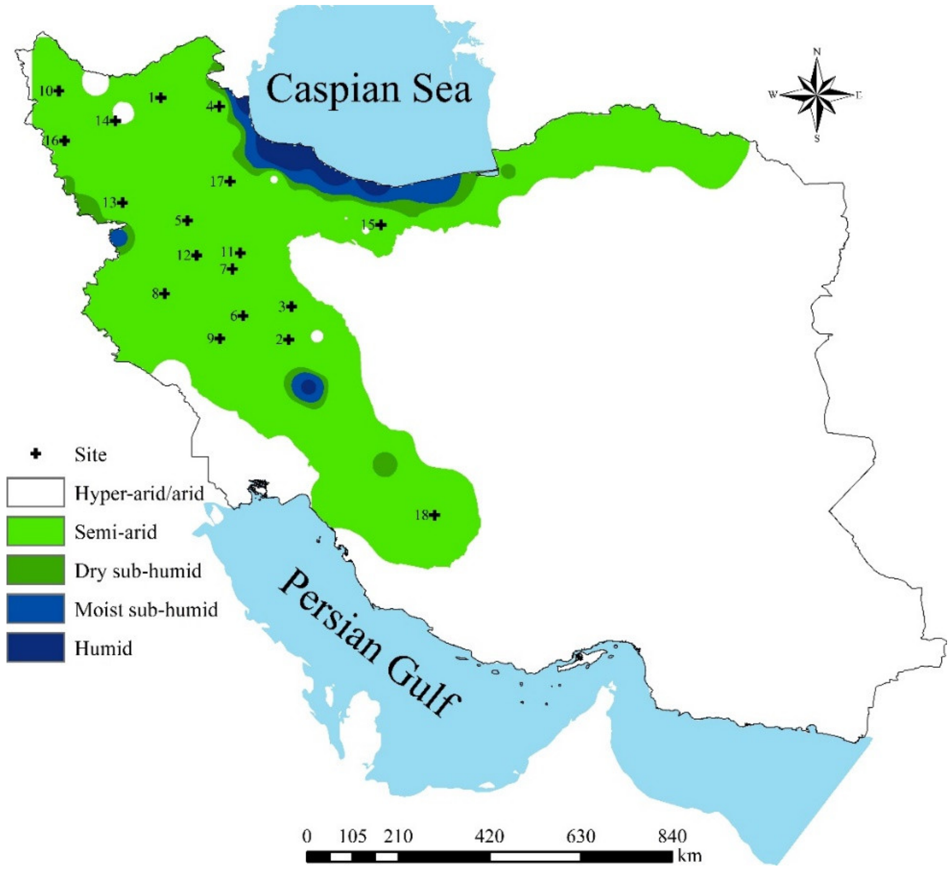

Figure 1. Location of the study sites with the number corresponding to the stations defined in Table 1. The climate classification is based on the aridity index (AI) proposed by UNEP [50]. The AI values of <0.05, 0.05–0.20, 0.20–0.50, 0.50–0.65, 0.65–1.00 and >1.00 represent the hyper-arid, arid, semi-arid, dry sub-humid, moist sub-humid and humid climatic regimes, respectively [50]. The AI was mapped by the Inverse Distance Weight (IDW) method.

The daily weather data including daily minimum and maximum temperature (recorded by a thermometer at height of 2 m, °C), wind speed (measured by an electronic anemometer at a height of 10 m, m s^{-1}), relative humidity (measured by hair hygrometer, %) and sunshine hours (recorded by an electronic pyranometer, hour) data were obtained from the Iran's Meteorological Organization (IRIMO) for the period of 1996–2016. The conversion of wind speed measured at 10 m height to wind speed at 2 m height was carried out according to Allen, et al. [19]. The sunshine hour measurements were converted to daily total solar radiation based on the Angstrom formula [19]. The easy-to-measure data for the dominant soil series at each site (i.e., particle size distribution, profile depth, soil organic carbon content, and soil bulk density) were obtained from the soil and land-use maps and reports provided by Iran's Soil and Water Research Institute (SWRI) (Table 2). Other soil-related inputs (i.e., lower limit of plant extractable soil water, LL, drained upper limit, DUL, saturated water content, θs, and saturated hydraulic conductivity, Ks) were determined based on the pedo-transfer functions established by Saxton, et al. [54] and Rawls, et al. [55] using the available soil physical characteristics for each site (Table 2). The agronomic management inputs, such as planting depth, method, distribution, spacing, and population were those reported by Nouri, et al. [56]. In addition, the cultivar coefficients of a bread winter wheat cultivar, i.e., Azar-2, as calibrated by Nouri, et al. [56] were used for model parameterization.

Table 2. Main soil physical properties of the study areas, averaged over all soil layers.

Site	Texture Class	Sand	Silt	Clay	OC	Depth	θ_s *	DUL *	LL *	ρ_b	Ks *
		%				cm		$cm^3\ cm^{-3}$		$g{\cdot}cm^{-3}$	$cm{\cdot}h^{-1}$
Ahar	clay loam	28.7	37.2	34.1	0.64	125	0.44	0.35	0.20	1.30	0.25
Aligodarz	loam	30.8	44.0	25.2	0.49	130	0.42	0.31	0.15	1.47	0.52
Arak	sandy clay loam	58.2	16.7	25.1	0.16	120	0.39	0.25	0.15	1.49	0.85
Ardebil	clay loam	27.8	43.1	29.1	0.44	120	0.43	0.33	0.18	1.27	0.37
Bijar	clay loam	27.7	39.9	32.4	0.56	150	0.45	0.35	0.21	1.31	0.28
Borojerd	loam	44.0	37.4	18.6	0.41	150	0.40	0.26	0.12	1.44	1.10
Hamedan	clay loam	32.4	29.6	38.0	0.40	120	0.44	0.36	0.23	1.40	0.20
Kermanshah	clay	30.4	28.0	41.6	1.30	120	0.47	0.41	0.26	1.32	0.12
Khorramabad	silty clay loam	14.2	52.0	33.8	0.50	125	0.47	0.38	0.21	1.30	0.17
Khoy	silt loam	20.4	54.5	25.1	0.36	150	0.48	0.32	0.16	1.19	0.53
Nozheh	clay loam	25.4	41.1	33.5	0.23	100	0.47	0.34	0.20	1.29	0.23
Qorveh	clay loam	25.8	34.6	39.6	0.27	150	0.46	0.37	0.24	1.34	0.18
Saghez	loam	31.7	45.9	22.4	0.55	130	0.39	0.23	0.09	1.48	1.27
Sahand	loam	47.2	31.9	20.9	0.35	130	0.40	0.26	0.13	1.45	1.15
Shemiran	clay loam	28.8	40.5	30.7	0.43	120	0.44	0.33	0.19	1.42	0.32
Urmia	sandy clay loam	52.4	21.4	26.2	0.80	120	0.38	0.25	0.15	1.45	0.82
Zanjan	sic	10.8	44.5	44.7	0.38	150	0.45	0.42	0.26	1.36	0.10
Zarghan	clay loam	27.2	43.1	29.7	0.19	120	0.43	0.33	0.17	1.39	0.36

Notes: * Determined based on the pedo-transfer functions. OC: Organic carbon content; θ_s: Saturated water content; DUL: Drained upper limit; LL: Lower limit of plant extractable soil moisture; ρ_b: Soil bulk density; K_s: Saturated hydraulic conductivity.

2.2. Modeling Framework

This study used the CSM-CERES-Wheat (Cropping System Model-Crop Environment Resource Synthesis-Wheat) provided in DSSAT v4.7.5 (Decision Support System for Agrotechnology Transfer) [57,58]. The model divides the growing period into nine phases and simulates crop growth and development based on genetic characteristics, solar radiation, photoperiod, atmospheric CO_2 concentration, and water and nitrogen availability. The CSM-CERES-Wheat uses the ET_P concept as it was established prior to the development of ET_o. Originally, the CSM-CERES-Wheat employs PT, as a model directly estimating ET_P. After developing DSSAT 4.0, PM, as a sophisticated ET_o model, was also included to estimate ET_P, known as the Penman-Monteith DSSAT. The DSSAT v4.7.5 uses the two-time step approach by multiplying a single crop coefficient with the PM-estimated ET_o:

$$ET_P = K_{cDSSAT} \times \frac{0.408\Delta(R_n - G) + \gamma(900/(T_{mean} + 273))u2(e_s - e_a)}{\Delta + \gamma(1 + 0.34u2)} \quad (1)$$

where Δ is the slope of saturation vapor pressure curve (kPa °C^{-1}), R_n is the net radiation at reference surface (MJ m^{-2} d^{-1}), G is the soil heat flux density (MJ m^{-2} d^{-1}) which is zero for daily analysis, T_{mean} is the daily mean air temperature at a height of 2 m (°C), u_2 is the average wind speed at a height of 2 m (m s^{-1}), e_s is the saturation vapor pressure (kPa), e_a is the actual vapor pressure (kPa), $e_s - e_a$ is the saturation vapor pressure deficit (kPa),

γ is the psychrometric constant, and K_{cDSSAT} stands for single crop coefficient for a given crop. The single crop coefficient (K_{cDSSAT}) is obtained in DSSAT as follows:

$$K_{cDSSAT} = 1.0 + (EORATIO - 1.0)\frac{LAI}{6.0} \quad (2)$$

where LAI stands for leaf area index (m^2 leaf/m^2 ground), and $EORATIO$ is a parameter specifically applied by DSSAT, not by FAO 56 method [19], which is equal to 1.0 for most crops (e.g., wheat and maize). Considering the value of 1.0 for EORATIO, the K_{cDSSAT} is equal to 1.0 (according to Equation (2)), and therefore, ET_o and ET_P estimated by PM can be used interchangeably in the CSM-CERES-Wheat [14]. As the CSM-CERES-Wheat is developed based on ET_P concept, we here used ET_P throughout the paper. It is noteworthy that, on the contrary to the DSSAT algorithm, the K_c value of wheat (and also the other crops) applied by the FAO 56 approach varies during a growing season.

The mathematical expression of the Priestley-Taylor/Ritchie equation (PT), the equation commonly used to calculate ET_P under weather data limitation, is:

$$ET_P = \begin{cases} 0.01 \times Exp\{0.18 \times (T_{\max} + 20.0)\} \times ET_{EQ} & if\ T_{\max} < 5.0 \\ 1.1 \times ET_{EQ} & if\ 5.0 \leq T_{\max} \leq 35.0 \\ \{([T_{\max} - 35.0] \times 0.05) + 1.1\} \times ET_{EQ} & if\ T_{\max} > 35.0 \end{cases} \quad (3)$$

$$ET_{EQ} = (SR \times 23.923) \times [2.04 \times 10^{-4} - (1.83 \times 10^{-4} \times Alb)] \times [29 + (0.6T_{\max} + 0.4T_{\min})] \quad (4)$$

$$Alb = \begin{cases} MSAlb & if\ LAI = 0.0 \\ 0.23 - (0.23 - MSAlb) \times Exp(-0.75 \times LAI) & if\ LAI > 0.0 \end{cases} \quad (5)$$

where T_{min} and T_{max} are minimum and maximum temperature (°C), respectively, LAI stands for leaf area index (m^2 leaf/m^2 ground), ET_{EQ} represents the equilibrium evapotranspiration (mm d^{-1}), SR is the solar radiation (MJ m^{-2} d^{-1}), Alb denotes the reflectance of soil-crop surface (fraction), and $MSAlb$ is the soil albedo with mulch and soil water effects (fraction).

The model then partitions ET_P into E_P (potential soil evaporation) and T_P (potential crop transpiration) based on leaf area index (LAI) and light extinction coefficient (K_{ext}):

$$E_P = ET_P \times Exp(-K_{ext} \times LAI) \quad (6)$$

$$T_P = ET_P \times (1 - Exp(-K_{ext} \times LAI)) \quad (7)$$

where E_P and T_P are potential and actual transpiration soil evaporation rate (mm d^{-1}), respectively, and K_{ext} is Light extinction coefficient, and LAI stands for leaf area index (m^2 leaf/m^2 ground).

The soil water subroutine of the CSM-CERES-Wheat applies the tipping bucket (cascade) approach considering upward flow through a layered soil profile based on water diffusivity. This subroutine, along with soil-plant-atmosphere interface energy balance module provides estimates of runoff, deep percolation, soil water movement, and evapotranspiration. The soil-plant-atmosphere interface energy balance subroutine simulates the potential root water uptake (PRWU) based on the plant root length density and soil physical properties using the microscopic uptake theory. The actual root water uptake (RWU) is then modeled as a function of soil water content for each layer. The PRWU is used for simulating actual transpiration (T) according to the following equation:

$$T_a = \begin{cases} Min(T_P, 10 \times PRWU) & if\ LAI > 10^{-4}\ and\ T_P > 10^{-4} \\ 0 & if\ LAI = 0\ and\ T_P = 0 \end{cases} \quad (8)$$

where T_a and T_P stand for actual and potential transpiration rate (mm d^{-1}), respectively, LAI is leaf area index (m^2 leaf/m^2 ground), and $PRWU$ denotes potential daily root water uptake over soil profile (cm d^{-1}).

The model computes a Soil Water stress Factor (SWFAC) to quantify the water deficit influences on crop growth, biomass related processes and phenology:

$$SWFAC = \begin{cases} PRWU/EP_1 = T_a/T_P & if\ PRWU < EP_1 \\ 1 & if\ PRWU \geq EP_1 \end{cases}$$
$$EP_1 = 0.1T_P \tag{9}$$

Moreover, another water stress index, namely the Turgor Factor (TURFAC), is also considered to determine the drought stress impacts on cell expansion:

$$TURFAC = \begin{cases} \frac{PRWU}{RWUEP_1 \times EP_1} = \frac{T_a}{RWUEP_1 \times T_P} & if\ \frac{PRWU}{EP_1} < RWUEP_1 \\ 1 \quad if\ \frac{PRWU}{EP_1} \geq RWUEP_1 \end{cases} \tag{10}$$

where T_a and T_P are, respectively, actual and potential transpiration rate (mm d^{-1}), respectively, LAI is leaf area index (m^2 leaf/m^2 ground), $RWUEP_1$d $PRWU$ stands for potential daily root water uptake over soil profile (cm d^{-1}).

The indices range from 0 for complete stress to 1 for no stress. The equations are all written based on the newest version of codes provided on https://github.com/DSSAT/dssat-csm-os (accessed on 1 June 2020). The ratio of T_a/T_P is also used in some other crop models such as CropSyst as the soil water stress [59]. The T_a/T_P ratio is proportional with the yield (Y) to maximum yield (Y_m) ratio according to Hanks [60], de Wit [61] and Paredes, et al. [62]. Note that in contrast with Y, T and T_P, the quantity of Y_m does not depend on the value of ET_P. Table 3 provides some of the meteorological and hydrological processes and conditions considered for the current scenario analysis.

Table 3. Crop modeling approach and inputs.

Process and Condition	Approach
Potential evapotranspiration (ET_P)	The Priestley-Taylor/Ritchie [28] and the Penman-Monteith DSSAT [19] equations
Potential evapotranspiration (ET_P) partitioning	The method provided by Ritchie (1972)
Actual soil evaporation	Physically-based model using diffusion theory proposed by Suleiman and Ritchie [63] and modified by Ritchie, et al. [64]
Root water uptake	Single root approach described in Ritchie [65] and Ritchie [66]
Actual crop transpiration	Limiting transpiration flow to actual root water absorption rate [66]
Runoff	Modified USDA-SCS CN [1] detailed in Williams, et al. [67]
Weather input data	Precipitation, near-surface wind speed (u_2), relative humidity, solar radiation, and minimum and maximum temperature (T_{min} and T_{max})
Drainage	Revised vertical drainage model proposed by Suleiman and Ritchie [63]
Soil moisture redistribution	Modified diffusivity theory [64]
Lower boundary condition	Free drainage
Simulation start date	30 days prior to sowing date

Notes: [1] United States Department of Agriculture-Soil Conservation Service Curve Number.

To assess the coupled stresses effects on determining the sensitivity of yield to the evapotranspiration accuracy, the simulations were conducted for two nitrogen levels and two water management levels. The scenarios were "rain-fed, high nitrogen stress", "rain-fed, low-nitrogen stress", "full irrigated, high nitrogen stress", and "full irrigated, low nitrogen stress". The rain-fed (no-irrigation) and full irrigated scenarios correspond to the high and low water stress conditions, respectively. The full irrigation scenario was based on the automatic irrigation module triggering when the available soil moisture dropped below 70% and was refilled back to its full capacity. The average Soil Water stress Factor (SWFAC) ranged from 0.33 to 0.51 for the rain-fed scenarios and >0.98 for the full irrigation scenarios. Two levels of urea application, i.e., 20 (high nitrogen stress) and 310 (low-nitrogen stress) kg ha^{-1}, were considered for the high and low-nitrogen stress scenarios, respectively. For the 20 kg ha^{-1} urea application, all nitrogen was applied during autumn at planting as recommended by the Iranian Dryland Agricultural Research Institute (DARI) and the Iran Ministry of Agriculture. For the 310 kg ha^{-1} urea application scenarios, 60 kg urea ha^{-1} was applied at planting and the remaining was equally split and applied within the phases of terminal spikelet to end of vegetation, end of vegetation to end of pre-anthesis ear growth, end of pre-anthesis ear growth to beginning of grain filling, and grain filling. In the current study, application of 310 kg ha^{-1} urea (according to the above-explained procedure) was found to cause a negligible nitrogen stress to plant, resembling a low-nitrogen stress condition. This urea application is not, however, common in wheat-growing regions in Iran. Nevertheless, it seems to be suitable for studying the coupled nitrogen-water stress effects on determining the errors in evapotranspiration estimates.

2.3. Statistical Evaluation

The difference magnitude or deviation (Δ) between the PT- and PM-estimated variables was obtained as follows:

$$\text{Deviation} = \frac{100}{\overline{X_{PM}}} \times \frac{\sum_{i=1}^{n} |X_{PT} - X_{PM}|}{n} \tag{11}$$

where X_{PT} and X_{PM} represent the estimates based on *PT* and *PM*, respectively, and *n* is the number of comparisons.

The non-parametric two-tailed Kolmogorov-Smirnov test was used to determine the change in distribution of ET_P and crop-related variables as a result of applying the two different ET_P methods (*PM* and *PT*). The Kolmogorov-Smirnov's D statistic is the largest deviation between two cumulative distribution curves (CDFs). The higher the Kolmogorov-Smirnov's statistic, the more significant the difference between CDFs. The significance of the difference between mean yield simulated by PT and PM was tested using the non-parametric Wilcoxon signed-rank test. The relationship between the variables was evaluated using the coefficient of determination (R^2).

3. Results and Discussion

3.1. The ET_P Deviations

The deviation in ET_P modeled based on PT and PM, averaged over four different scenarios, across a wide range of u_2 during the growing season is depicted in Figure 2. It shows that the difference in ET_P estimates increases linearly with an increase in u_2 from 1.3 to 3.5 m s^{-1}. The deviation of ET_P estimates was less than 12.0% within the u_2 range of 1.3–2.0 m s^{-1} implying a closer performance of PT to PM. Cristea, et al. [68] also stated that PT provides a more reliable fit when u_2 is less than 2.0 m s^{-1}. Nouri and Homaee [46] also concluded that deviation of u_2 from the range of 1.5–2.5 m s^{-1} leads to a large error in estimating ET_o under data scarcity. The ET_P estimated by PT deviated from PM-estimated ET_P by more than 15% in our studied regions with a growing season u_2 greater than 2.45 and less than 1.0 m s^{-1}. As expected, the largest deviation in ET_P estimates was observed for the windy environments. For four surveyed windy sites that had a u_2 above 3.0 m s^{-1} (Bijar, Aligodarz, Sahand and Ardebil), the difference between ET_P estimates was larger than 19.0%. The modeling literature also warns against not taking u_2 into consideration for application of crop models for high wind speed locations [45,46,69–71].

3.2. Deviations in Crop-Related Variables

The deviation of evaporation (E_a) and transpiration (T_a) increased linearly with an increase in the deviation of PT-estimated ET_P from PM-estimated ET_P for all scenarios (Figure 3). The average deviations in transpiration and evaporation were 6.0% and 7.8%, respectively, under "rain-fed, low-nitrogen stress", 4.8% and 5.6% under "rain-fed, high nitrogen stress", 14.0% and 11.1% under "full irrigation, low nitrogen stress", and 13.9% and 10.4% under "full irrigation, high nitrogen stress". Given a smaller deviation for evaporation and transpiration for no-irrigation scenarios, PT was similar to PM in simulating evapotranspiration components under drier condition (Figure 3). Furthermore, the availability of nitrogen does not seem to contribute significantly to the deviation in the estimated evapotranspiration components. The difference for evapotranspiration components under rain-fed scenarios for the study sites was below 13% (Figure 3a–d). However, the difference between PT-simulated transpiration from the transpiration simulated based on PM was more than 20% under full irrigation scenarios for the four windy sites, i.e., Sahand, Ardebil, Aligodarz and Bijar with u_2 above 3 m s^{-1} (Figure 3e,g). The evaporation results demonstrated a difference ranging from 12.8% to 19.2% for the sites with u_2 values larger than 3 m s^{-1} for low water stress (full irrigation) scenarios (Figure 3f,h). It can be concluded that the difference between evapotranspiration components obtained by PT and PM is less under severe soil drought. However, PT may not be reliable for estimating the evapotranspiration components, particularly transpiration, for windy areas under full irrigation when u_2 data are missing.

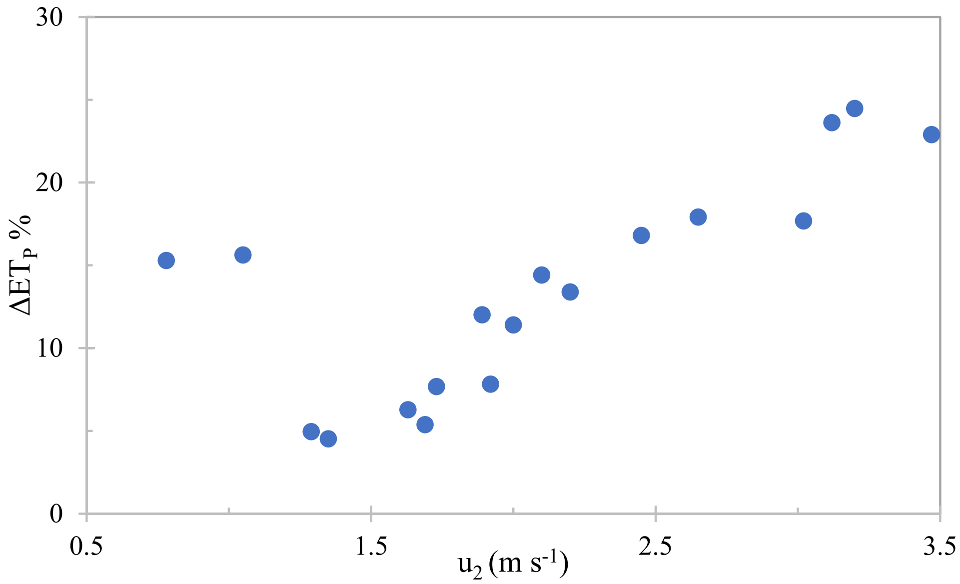

Figure 2. The average deviation of Priestley-Taylor/Ritchie (PT)-estimated potential evapotranspiration (ET_P) from Penman-Monteith DSSAT-estimated ET_P (Δ%) over a range of near-surface wind speeds (u_2) during the wheat growing season for four different management scenarios.

Under “rain-fed, low-nitrogen stress”, the difference between grain yield, T_a/T_P and maximum LAI (LAI_m) estimated by PM and PT increased linearly by increasing the difference in ET_P estimates (Figure 4a–c). The difference exceeded 26.0% for yield, 16.0% for T_a/T_P, and 38.0% for LAI_m under “rain-fed, low-nitrogen stress” for the four windy sites with u_2 above 3 m s^{-1} (Figure 4a–c). Considerable the difference between T_P partitioned from PT-estimated ET_P and that partitioned from PM-estimated ET_P seems to arise from the large difference between LAI and ET_P simulations (Equation (7)) for the windy sites under “rain-fed, low-nitrogen stress”. Thus, despite a relatively small difference between the transpiration estimates (13.0% >), PT-estimated T_P deviated greatly from PM-estimated T_P leading to a high difference in T_a/T_P simulations under “rain-fed, low-nitrogen stress” (16.0% <). In other words, a high deviation of ET_P estimates causes a large difference in T_P (Equation (7)) and, consequently, in the water stress index (Equations (9) and (10)). Given that the correlation coefficient was greater than 0.65 (Figure 5), there exists a strong association between the difference of T_a/T_P and the difference in yield under high water stress conditions. It is noteworthy that there is a direct association between T_a/T_P and yield [62]. Consequently, a large difference in T_a/T_P estimates resulted in a large difference in wheat yield for the sites that had a high wind speed and where soil water was highly restricted but with sufficient nitrogen. Liu, et al. [72] also reported that the application of different ET_P approaches impacts the accuracy of yield simulations by affecting transpiration and potential transpiration results for water-stressed soils. PT-simulated daily LAI was substantially different from PM-simulated daily LAI for the "rain-fed, low-nitrogen stress" scenario leading to a relatively high difference in estimating T_a/T_P based on PT and PM for the growing season that had a u_2 of 3.50 m s^{-1} (Figure 6a,e). In this case, there was a 37.1% difference in the daily LAI and a 13.4% difference in the daily T_a/T_P results.

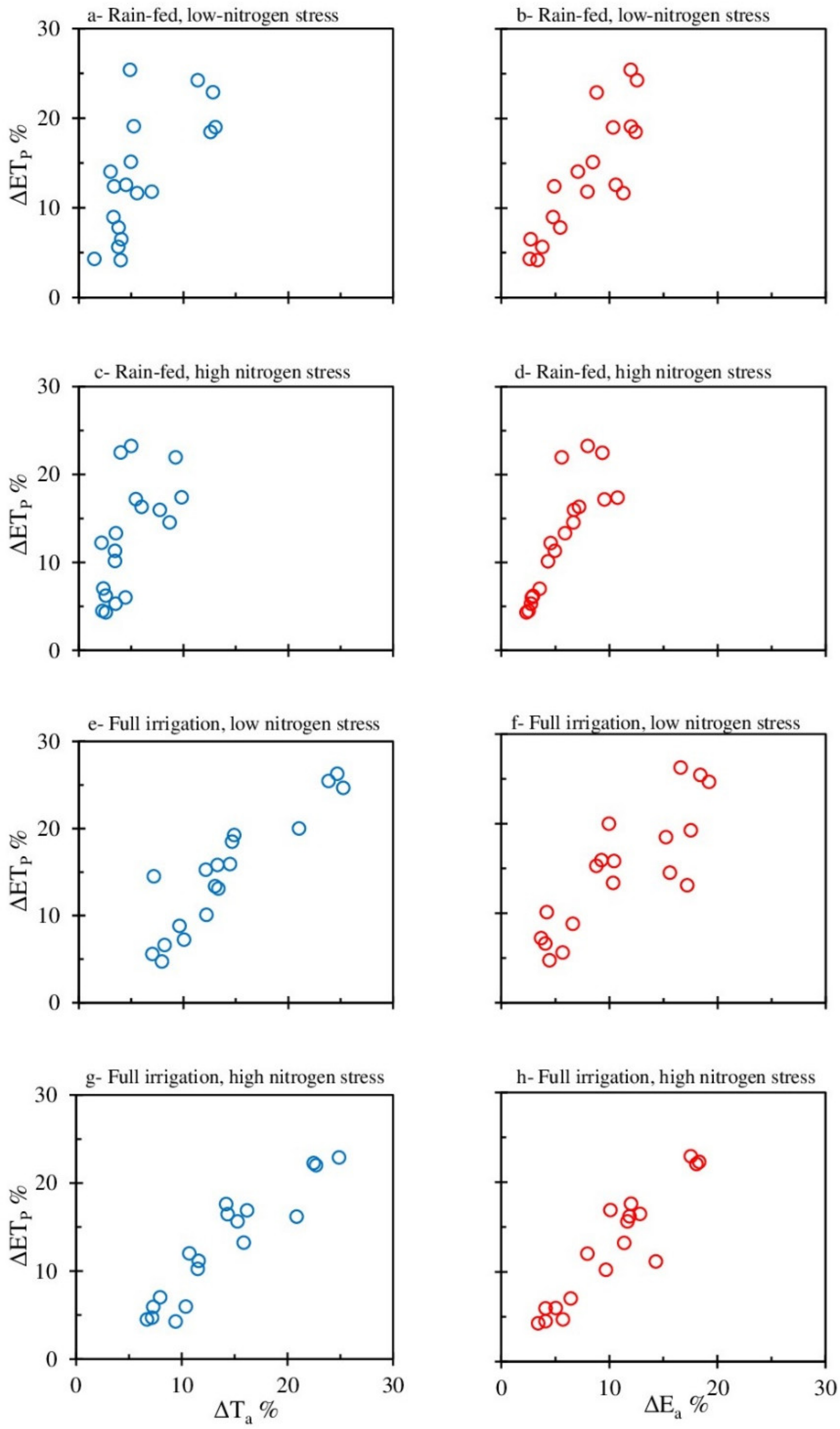

Figure 3. The deviation of potential evapotranspiration (ΔET_P) against deviation of soil evaporation (ΔE_a) and transpiration (ΔT_a) simulated based on the Priestley-Taylor/Ritchie and the Penman-Monteith-DSSAT methods.

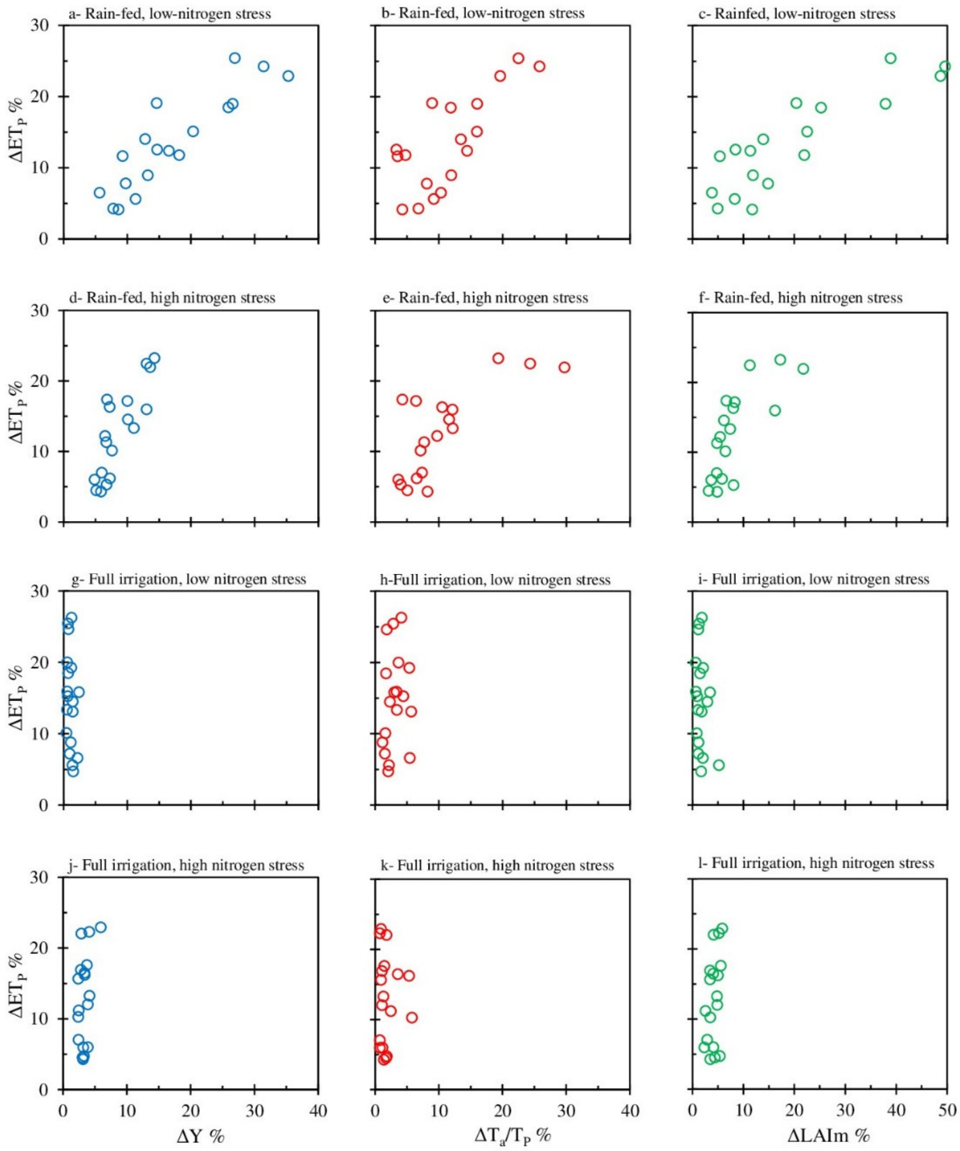

Figure 4. The deviation of potential evapotranspiration (ΔET_P) against deviation of yield (ΔY), maximum Leaf Area Index (ΔLAI_m) and actual transpiration to potential transpiration ratio ($\Delta T_a/T_P$) simulated by using the Priestley-Taylor/Ritchie and the Penman-Monteith DSSAT.

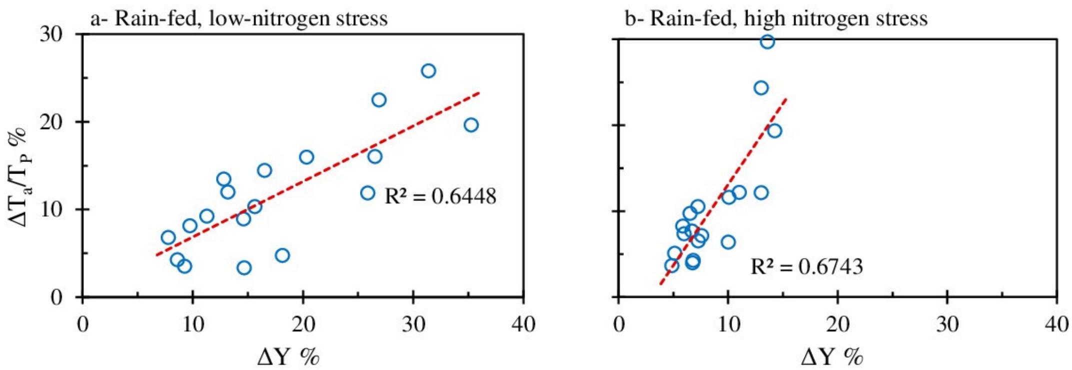

Figure 5. The association between the deviation in actual transpiration to potential transpiration ($\Delta T_a/T_P$) and yield (ΔY) simulated based on the Priestley-Taylor/Ritchie and the Penman-Monteith DSSAT under rain-fed scenarios.

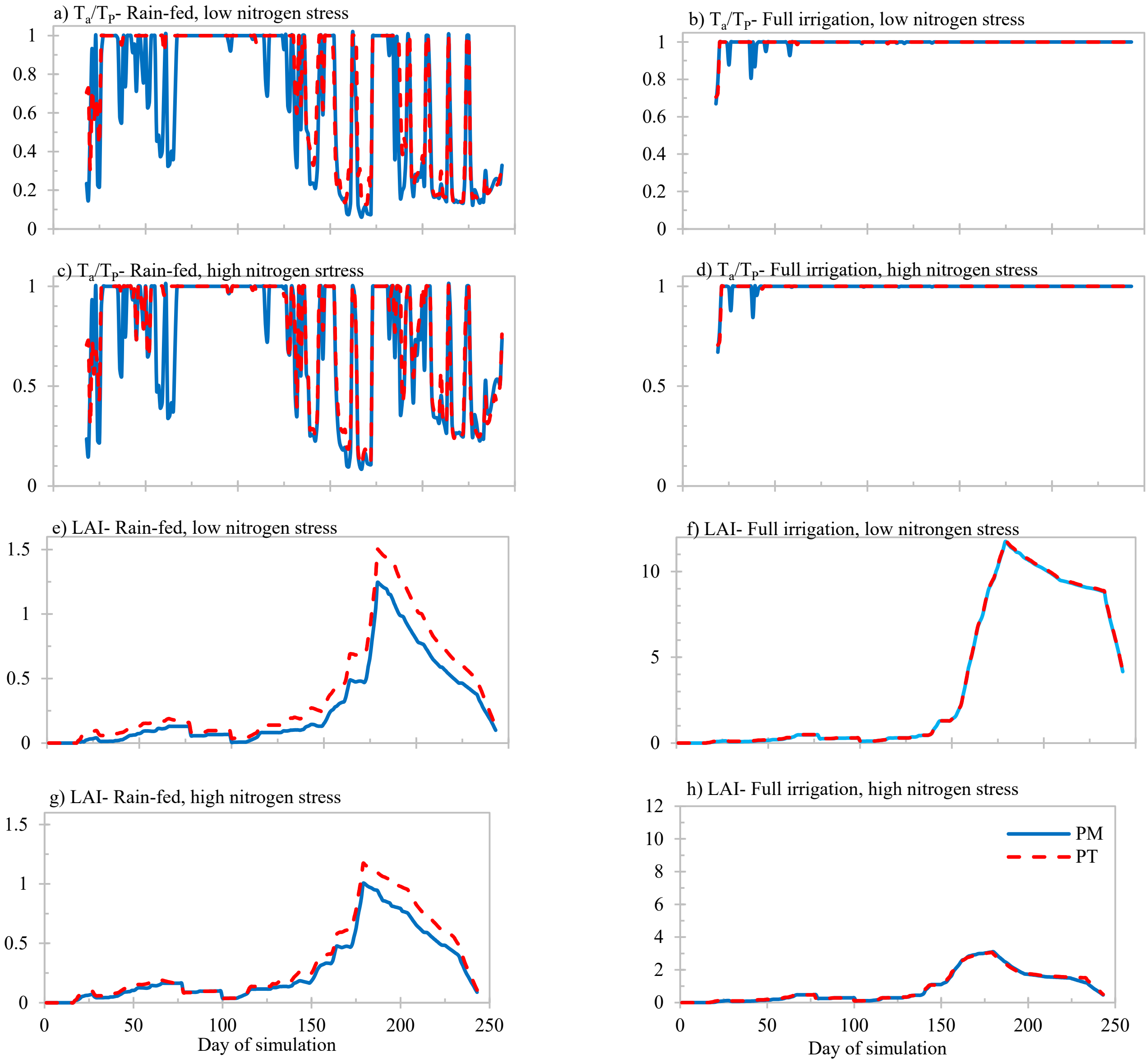

Figure 6. The daily Leaf Area Index (LAI) and actual transpiration to potential transpiration (T_a/T_P) ratio simulated by the Priestley-Taylor/Ritchie (PT) and the Penman-Monteith DSSAT (PM) during the 1999–2000 growing season with near-surface wind speeds (u_2) of 3.50 m s^{-1} at Ardebil site under the water-nitrogen stress scenarios.

The statistically significant difference in distribution of PM- and PT-estimated ET_P at 89% for the study sites is shown in Table 4. The distribution of PT-estimated T_a/T_P differed significantly from the PM-estimated T_a/T_P for only four windy cases under "rain-fed, low-nitrogen stress". Moreover, the difference in ET_P distribution led to a significant difference in LAI_m distribution for three windy sites, i.e., Aligodarz, Bijar, and Sahand, based on the Kolmogorov-Smirnov test under "rain-fed, low-nitrogen stress" scenario. However, wheat yield was significantly different ($p < 0.05$) based on PM and PT only for one windy case (Bijar) under the no-irrigation and low-nitrogen stress condition.

The Wilcoxon signed-rank test detected a significant difference ($p < 0.05$) between PT- and PM-simulated yield means for 89% of surveyed locations for the scenario of "rain-fed, low-nitrogen stress" (Figure 7a). The average PM-simulated yield of 1812 kg ha^{-1} and PT-simulated yield of 2034 kg ha^{-1} were found under "rain-fed, low-nitrogen stress" condition. This difference can be ascribed to the fact that PM considers wind speed impacts, resulting in a higher atmospheric evaporative power and water stress, and consequently a lower rain-fed yield particularly for windy areas. The average deviations in minimum, 25th percentile (or first quartile, q_1), median (or second quartile, q_2), 75th percentile (or third quartile, q_3), and maximum of yield modeled by employing PM and PT were 108, 207, 313, 346, and 372 kg ha^{-1}, respectively, under "rain-fed, low-nitrogen stress" scenario (Figure 7a). The difference between the minimum, q_1, q_2 (median), q_3, and maximum of PT- and PM-simulated yield was 97, 286, 515, 617, and 952 kg ha^{-1}, respectively, on average for the four windy cases under "rain-fed, low-nitrogen stress" condition. Thus, the difference in ET_P estimates resulted in a larger difference for simulated yield that was above the median yield for the windy cases under "rain-fed, low-nitrogen stress". Therefore, it seems that the difference in rain-fed yield as a result of deviation in ET_P estimates is more pronounced for wetter years when a higher yield is expected under rain-fed conditions.

Table 4. The Kolmogorov-Smirnov D statistic obtained for yield, maximum Leaf Area Index (LAI_m), actual transpiration to potential transpiration ratio (T_a/T_P), and potential evapotranspiration (ET_P) under water-nitrogen stress scenarios.

Site	Rain-Fed, Low-Nitrogen Stress			Rain-Fed, High Nitrogen Stress			Full Irrigation, Low Nitrogen Stress			Full Irrigation, High Nitrogen Stress			ET_P
	Yield	T_a/T_P	LAI_m	Yield	T_a/T_P	LAI_m	Yield	T_a/T_P	LAI_m	Yield	T_a/T_P	LAI_m	
Ahar	0.25	0.25	0.35	0.20	0.35	0.35	0.10	0.20	0.10	0.20	0.25	0.20	**1.00**
Aligodarz	0.30	**0.45**	**0.40**	0.20	0.35	0.10	0.15	0.55	0.10	0.20	0.15	0.20	**1.00**
Arak	0.20	0.20	0.10	0.15	0.20	0.15	0.10	0.30	0.05	0.15	0.35	0.10	0.15
Ardebil	0.25	**0.45**	0.30	0.25	0.35	0.25	0.10	0.35	0.10	0.20	0.15	0.15	**0.90**
Bijar	**0.45**	**0.50**	**0.45**	0.30	0.45	0.30	0.15	0.45	0.10	0.20	0.15	0.15	**1.00**
Borojerd	0.35	0.30	0.30	0.15	0.35	0.20	0.10	0.35	0.10	0.15	0.35	0.15	**1.00**
Hamedan	0.15	0.25	0.25	0.15	0.25	0.10	0.15	0.20	0.15	0.15	0.35	0.20	**0.50**
Kermanshah	0.25	0.35	0.20	0.25	0.15	0.15	0.10	0.15	0.10	0.10	0.20	0.05	**0.80**
Khorramabad	0.15	0.35	0.15	0.15	0.25	0.15	0.10	0.25	0.05	0.15	0.15	0.15	**0.50**
Khoy	0.10	0.10	0.10	0.15	0.10	0.10	0.15	0.20	0.15	0.10	0.30	0.20	**0.20**
Nozheh	0.10	0.35	0.25	0.20	0.30	0.20	0.15	0.15	0.05	0.25	0.30	0.10	**0.75**
Qorveh	0.20	0.20	0.25	0.25	0.25	0.10	0.10	0.20	0.10	0.20	0.35	0.25	**0.95**
Saghez	0.15	0.25	0.20	0.15	0.25	0.10	0.05	0.20	0.10	0.10	0.20	0.10	**0.50**
Sahand	0.30	**0.45**	**0.55**	0.35	**0.50**	**0.45**	0.10	0.35	0.10	0.10	0.35	0.10	**0.95**
Shemiran	0.15	0.15	0.10	0.10	0.25	0.20	0.15	0.20	0.10	0.15	0.35	0.15	**0.85**
Urmia	0.15	0.20	0.20	0.15	0.25	0.10	0.10	0.25	0.15	0.10	0.25	0.05	**0.60**
Zanjan	0.25	0.35	0.30	0.20	0.20	0.15	0.10	0.20	0.10	0.20	0.15	0.15	**0.70**
Zarghan	0.25	0.15	0.25	0.25	0.30	0.25	0.10	0.15	0.10	0.10	0.35	0.15	**0.90**

Notes: The values in bold indicate significant differences at the level of 95%.

The difference in magnitude, averaged over all study sites, dropped from 17.7% to 8.7% for grain yield, from 11.7% to 10.5% for T_a/T_P, and from 20.5% to 8.4% for LAI_m by decreasing the applied urea from 310 (low-nitrogen stress) to 20 (high nitrogen stress) kg ha^{-1} under rain-fed condition (Figure 4d–f). Compared to "rain-fed, low-nitrogen stress" condition, there was a smaller difference between PT- and PM-simulated yields due to a smaller difference in the estimates for LAI and T_a/T_P under "rain-fed, high nitrogen stress". There was a 14.3% and 4.2% decrease in the difference of PT-simulated daily LAI and T_a/T_P from PM-simulated daily LAI and T_a/T_P, respectively, by reducing the nitrogen application rate from 310 (low-nitrogen stress) to 20 (high nitrogen stress) kg urea ha^{-1} under no-irrigation condition for the given windy growing season (Figure 6a,c,e,g). The difference in ET_P did not significantly change the distribution of T_a/T_P, LAI_m and yield under "rain-fed-high nitrogen stress" scenario for majority of the cases (Table 4). The difference in mean crop yield was statistically significant ($p < 0.05$) for two-third of the cases based on the Wilcoxon signed-rank test for "rain-fed, high nitrogen stress" scenario (Figure 7b). On average, a deviation of 50, 42, 50, 50, and 41 kg ha^{-1} was obtained for minimum, q_1, q_2 (median), q_3, and maximum of the simulated yield based on PM and PT, respectively, under "rain-fed, high nitrogen stress" condition (Figure 7b). For the four windy cases, the difference of minimum, q_1, q_2 (median), q_3, and maximum was 60, 77, 91, 25, and 26 kg ha^{-1}, respectively, under "rain-fed, high nitrogen stress" scenario. Therefore, the difference in below-median simulated yield was larger for the windy areas under severe water-nitrogen stress.

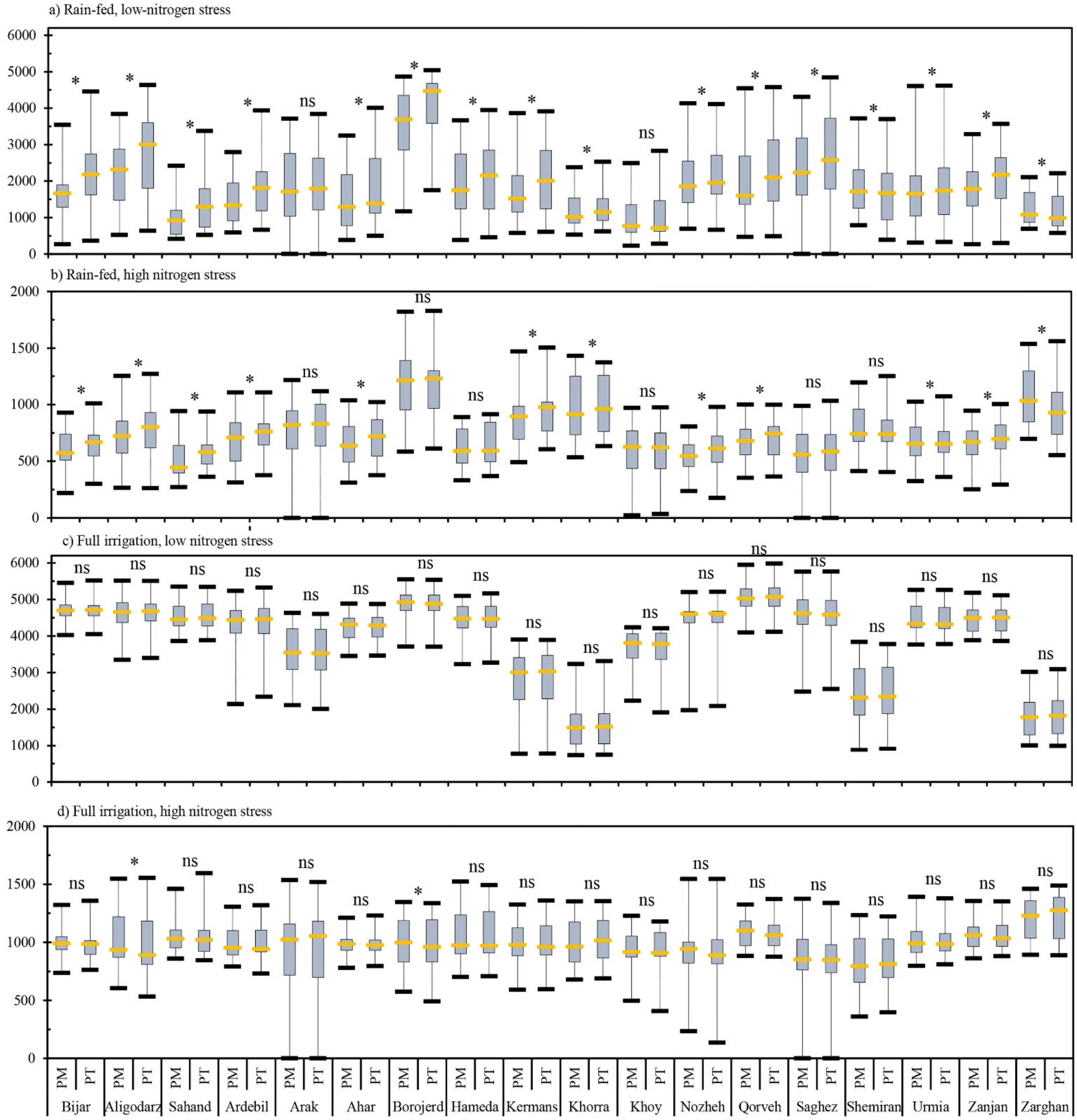

Figure 7. Distribution of crop yield (kg ha^{-1}) simulated by applying the Priestley-Taylor/Ritchie (PT) and the Penman-Monteith DSSAT (PM) for four different management scenarios of all studied sites. The asterisks (*) indicate significant differences at the level of 95%. The "ns" indicates statistically insignificant differences. The boxes boundaries indicate the 25th and 75th percentiles, the lines within the boxes mark the median and the inner and outer fences represent the minimum and maximum values, respectively.

The yield, T_a/T_P and LAI_m based on PT deviated from the PM-simulated by less than 6.0% (average across all sites) for the full irrigation scenarios (Figure 4g–l). Despite the high deviation for transpiration (<20%), the difference between PT- and PM-simulated LAI_m and T_a/T_P ranged from 0.75% to 5.8% under full irrigation for the windy environments (Figure 4h,i,k,l) where the performance of PT differed noticeably from PM (Figure 2).

The average difference between yield obtained by using PM and PT was statistically insignificant ($p > 0.05$) for the majority of cases for the full irrigation scenarios (Figure 7c,d). Moreover, the difference in the distribution of T_a/T_P, LAI_m and yield was insignificant under low water stress (Table 4). When there is sufficient soil moisture for root water uptake, transpiration approaches potential transpiration and T_a/T_P is close to its maximum value of 1. A small difference in the estimates for LAI and T_a/T_P resulted in a small difference in yield when there was sufficient water available for root water uptake. In other words, despite quite a large difference (above 17.0%) obtained for PT-estimated ET_P and transpiration for the high wind speed areas (Figures 2 and 3), there was a low difference (below 6.0%) in wheat yield and T_a/T_P under full irrigation scenarios. For the windy growth period (Figure 6), the PT-simulated daily LAI and T_a/T_P differed from the PM-simulated daily LAI and T_a/T_P by less than 1.8% under full irrigation (Figure 6b,d,f,h). Hence, different ET_P modeling methods do not seem to result in notable differences in yield when the available water is not restricted. It also seems that nitrogen limitation does not appear to make a significant contribution to yield deviation when water is not severely limited.

Overall, the simulated yield does not appear to be notably sensitive to the difference in the estimated ET_P when soil moisture is replenished adequately. For locations where irrigation and/or precipitation meet crop demand, the difference of the estimates for ET_P is unlikely to cause notable differences in predicted yield. The deviation in the estimates for ET_P is, however, of major importance for the prediction of yield when the soil moisture availability (as the only limiting factor) is severely limited. Hence, when u_2 surpasses 3 m s^{-1} and a drought occurs, resembling the condition of dry farming for windy semi-arid/arid sites, and other requirements such as nitrogen are met, simulating crop growth, development and yield based on the ET_P method that does not consider wind dynamics such as PT is expected to be associated with large uncertainties. This is mainly due to the fact that a large difference in the estimates for ET_P results in a high deviation for LAI, the water stress index (T_a/T_P) and yield predictions for water-stressed windy environments. A limitation in nitrogen can reduce the sensitivity of simulating yield to the difference in ET_P estimates for windy fields that experience a severe soil moisture shortage.

As stated previously, we applied the Angstrom equation to approximate solar radiation, as it is not directly measured in our study area. This might add some uncertainties to the results, linked to the coefficient of the formula. In this study, DSSAT was forced by the solar radiation estimated by the Angstrom equation for both cases of using PT and PM. As a result, comparing the results produced by PM and PT is likely to eliminate the uncertainties related to the solar radiation estimates.

The most recent source code for the Cropping System Model (CSM) of DSSAT includes five ET_P modeling frameworks namely the Penman-Monteith DSSAT (dynamic and default formats) [19], the standardized ASCE Penman-Monteith (ASCE-PM, for short and tall reference crop) [27], the standard reference evaporation calculation for inland south eastern Australia [73], Penman FAO 24 [74], and Priestley-Taylor/Ritchie [28]. Except for the Priestley-Taylor/Ritchie equation, the other alternatives require at least four sets of data including vapor pressure deficit (VPD), wind speed, temperature (minimum and maximum), and solar radiation (or sunshine hour). Therefore, there is only one method for estimating ET_P in DSSAT that does not require wind speed as input. Including additional ET_P equations in CSM such as Hargreaves-Samani [29] may decrease the uncertainty linked to the model structure under data scarcity. Consequently, there is a need for further studies to address the performance of additional ET_P equations in simulating crop yield by using incomplete datasets under extreme climatic conditions.

The uncertainty related to the parameters can be also reduced by fitting the empirical coefficients of ET_P equations against PM-modeled ET_P values for windy conditions [69,75]. However, updating the coefficients needs complete weather data to determine ET_P based on PM which are not often available for data-scarce locations [46,75]. In addition, recalibration of empirical coefficients is highly spatially dependent. Ravazzani, et al. [76] stated that the readjustment of ET_P formulae's coefficients may even depreciate the goodness of fit for other geographic or climatic conditions. Additionally, this technique depends on the time period used, particularly under current climate change and variability [46]. Consequently, adjusting coefficients to reduce the parameter-related uncertainties may not sufficiently be reliable for application to other locations and time periods. The other approaches such as updating the empirical coefficients based on the u_2 observations [77], and application of constant or local average u_2 values [78–80] have also been adopted in windy data-poor areas. However, the accuracy of such approaches is questionable in windy areas with high u_2 variance, particularly in daily resolution required by crop models [78].

In this study, we focused only on the influence of ET_P sub-models' selection on final yield predictions across a wide range of wind speed conditions. However, as two different soil evaporation sub-models, Ritchie-Ceres and Suleiman-Ritchie, are included in DSSAT, selecting different ET_P-soil evaporation sub-model combinations may affect yield modeling [14]. Hence, the sensitivity of different combinations of soil evaporation-ET_P sub-models to climatic data limitation has to be evaluated in future studies.

The radiation-based ET_P alternatives, e.g., PT have been commonly used for projecting crop response to future climate changes [81–84] as especially the temperature products of GCMs (General Climate models) are more reliable with respect to wind speed and relative humidity outputs required to calculate ET_P based on more physically-based approaches such as PM [85–87]. For windy conditions, however, there are significant uncertainties when temperature- or radiation-based models are used for projecting the future climate change-induced changes in the soil-plant-atmosphere systems. Special care must be taken to select the most appropriate ET_P model for climate change impact assessments at windy sites so as to provide reasonable projections needed by policy-makers.

4. Conclusions

In this study we determined the importance of potential evapotranspiration (ET_P) estimation for crop modeling accuracy under data limitation across a wide range of wind speeds. Therefore, the difference between wheat yield predicted by the CSM-CERES-Wheat run based on the Priestley-Taylor/Ritchie (PT) and the Penman-Monteith DSSAT (PM) was determined. We found that the difference between yield simulated based on PT and PM was larger than 26% and statistically significant ($p < 0.05$) at the studied areas with u_2 (wind speeds at 2 m height) above 3 m s^{-1} under "rain-fed, low-nitrogen stress" condition. This is explainable by large differences for LAI and actual transpiration to potential transpiration ratio or water stress index (T_a/T_P) estimates leading to a large difference in predicted yield by employing different ET_P equations at windy sites for this condition. The difference in estimated ET_P resulted in a significant difference in distribution of maximum LAI and T_a/T_P at windy cases under "rain-fed, low-nitrogen stress" condition. However, only one case with high wind speed displayed a significant deviation in distribution of yield as a consequence of deviation in ET_P estimates under "rain-fed, low-nitrogen stress". When soil moisture is considerably constrained, nitrogen deficiency decreases the deviation in LAI_m, T_a/T_P and yield simulated by use of different ET_P equations. The yield deviation was below 6% and statistically insignificant ($p > 0.05$) for full irrigation scenarios. This can be attributed to low difference in LAI and T_a/T_P estimates. The distribution of LAI_m, T_a/T_P and yield simulations deviated insignificantly under full irrigation condition. Nitrogen availability is unlikely to affect the yield results accuracy under full irrigation condition. Overall, the ET_P estimation using datasets lacking u_2 would lead to erroneous crop yield predictions under dry farming across windy environments. The difference in ET_P estimation seems, however, not to notably affect the accuracy of predicted yield when the soil moisture is adequate.

Author Contributions: M.N. conceptualized the methodology framework, validated the results and was a major contributor in writing the manuscript. G.H. revised the original draft and contributed in methodology, data analysis, and visualization. M.B. provided the required resources, and edited and proofread the main text. M.H. analyzed and validated the data, and contributed in editing the manuscript. All authors have read and agreed to the published version of the manuscript.

Funding: This research received no external funding.

Institutional Review Board Statement: Not applicable.

Informed Consent Statement: Not applicable.

Data Availability Statement: The data presented in this study are available on request from the corresponding author.

Conflicts of Interest: The authors declare no competing interests.

References

1. Brauman, K.A.; Siebert, S.; Foley, J.A. Improvements in crop water productivity increase water sustainability and food security—A global analysis. *Environ. Res. Lett.* **2013**, *8*, 024030. [CrossRef]
2. Richter, B.D.; Brown, J.D.; DiBenedetto, R.; Gorsky, A.; Keenan, E.; Madray, C.; Morris, M.; Rowell, D.; Ryu, S. Opportunities for saving and reallocating agricultural water to alleviate water scarcity. *Water Policy* **2017**, *19*, 886–907. [CrossRef]
3. Scott, C.A.; Vicuña, S.; Blanco-Gutiérrez, I.; Meza, F.; Varela-Ortega, C. Irrigation efficiency and water-policy implications for river basin resilience. *Hydrol. Earth Syst. Sci.* **2014**, *18*, 1339–1348. [CrossRef]
4. Boote, K.J.; Jones, J.W.; Pickering, N.B. Potential Uses and Limitations of Crop Models. *Agron. J.* **1996**, *88*, 704–716. [CrossRef]
5. Jones, J.W.; Antle, J.M.; Basso, B.; Boote, K.J.; Conant, R.T.; Foster, I.; Godfray, H.C.J.; Herrero, M.; Howitt, R.E.; Janssen, S.; et al. Brief history of agricultural systems modeling. *Agric. Syst.* **2017**, *155*, 240–254. [CrossRef] [PubMed]
6. Jin, X.; Kumar, L.; Li, Z.; Feng, H.; Xu, X.; Yang, G.; Wang, J. A review of data assimilation of remote sensing and crop models. *Eur. J. Agron.* **2018**, *92*, 141–152. [CrossRef]
7. Seidel, S.J.; Palosuo, T.; Thorburn, P.; Wallach, D. Towards improved calibration of crop models – Where are we now and where should we go? *Eur. J. Agron.* **2018**, *94*, 25–35. [CrossRef]
8. Tan, J.; Cui, Y.; Luo, Y. Assessment of uncertainty and sensitivity analyses for ORYZA model under different ranges of parameter variation. *Eur. J. Agron.* **2017**, *91*, 54–62. [CrossRef]
9. Wallach, D.; Makowski, D.; Jones, J.W.; Brun, F. Chapter 6—Uncertainty and Sensitivity Analysis. In *Working with Dynamic Crop Models*, 3rd ed.; Wallach, D., Makowski, D., Jones, J.W., Brun, F., Eds.; Academic Press: New York, NY, USA, 2019; pp. 209–250.
10. Yan, L.; Jin, J.; Wu, P. Impact of parameter uncertainty and water stress parameterization on wheat growth simulations using CERES-Wheat with GLUE. *Agric. Syst.* **2020**, *181*, 102823. [CrossRef]
11. Niu, X.; Easterling, W.; Hays, C.J.; Jacobs, A.; Mearns, L. Reliability and input-data induced uncertainty of the EPIC model to estimate climate change impact on sorghum yields in the U.S. Great Plains. *Agr. Ecosyst. Environ.* **2009**, *129*, 268–276. [CrossRef]
12. Fodor, N.; Kovács, G.J. Sensitivity of crop models to the inaccuracy of meteorological observations. *Phys. Chem. Earth Parts A B C* **2005**, *30*, 53–57. [CrossRef]
13. de Wit, A.J.W.; Boogaard, H.L.; van Diepen, C.A. Spatial resolution of precipitation and radiation: The effect on regional crop yield forecasts. *Agric. For. Meteorol.* **2005**, *135*, 156–168. [CrossRef]
14. Thorp, K.R.; Marek, G.W.; DeJonge, K.C.; Evett, S.R. Comparison of evapotranspiration methods in the DSSAT Cropping System Model: II. Algorithm performance. *Comput. Electron. Agric.* **2020**, *177*, 105679. [CrossRef]
15. DeJonge, K.C.; Thorp, K.R.; Marek, G.W. The apples and oranges of reference and potential evapotranspiration: Implications for agroecosystem models. *Agric. Environ. Lett.* **2020**, *5*, e20011. [CrossRef]
16. Kite, G.W.; Droogers, P. Comparing evapotranspiration estimates from satellites, hydrological models and field data. *J. Hydrol.* **2000**, *229*, 3–18. [CrossRef]
17. Xie, H.; Zhu, X. Reference evapotranspiration trends and their sensitivity to climatic change on the Tibetan Plateau (1970–2009). *Hydrol. Processes* **2013**, *27*, 3685–3693. [CrossRef]
18. Xiang, K.; Li, Y.; Horton, R.; Feng, H. Similarity and difference of potential evapotranspiration and reference crop evapotranspiration—A review. *Agric. Water Manag.* **2020**, *232*, 106043. [CrossRef]
19. Allen, R.G.; Pereira, L.S.; Raes, D.; Smith, M. *Crop Evapotranspiration-Guidelines for Computing Crop Water Requirements—FAO Irrigation and Drainage Paper 56*; Food and Agriculture Organization of the United Nations: Rome, Italy, 1998; p. 326.
20. Corbari, C.; Ravazzani, G.; Galvagno, M.; Cremonese, E.; Mancini, M. Assessing Crop Coefficients for Natural Vegetated Areas Using Satellite Data and Eddy Covariance Stations. *Sensors* **2017**, *17*, 2664. [CrossRef]
21. Thorp, K.R.; DeJonge, K.C.; Marek, G.W.; Evett, S.R. Comparison of evapotranspiration methods in the DSSAT Cropping System Model: I. Global sensitivity analysis. *Comput. Electron. Agric.* **2020**, *177*, 105658. [CrossRef]
22. Sau, F.; Boote, K.J.; Bostick, W.M.; Jones, J.W.; Mínguez, M.I. Testing and Improving Evapotranspiration and Soil Water Balance of the DSSAT Crop Models. *Agron. J.* **2004**, *96*, 1243–1257. [CrossRef]
23. López-Cedrón, F.X.; Boote, K.J.; Piñeiro, J.; Sau, F. Improving the CERES-Maize Model Ability to Simulate Water Deficit Impact on Maize Production and Yield Components. *Agron. J.* **2008**, *100*, 296–307. [CrossRef]
24. Nouri, M.; Homaee, M. Reference crop evapotranspiration for data-sparse regions using reanalysis products. *Agric. Water Manage.* **2022**, *262*, 107319. [CrossRef]
25. Garcia y Garcia, A.; Guerra, L.C.; Hoogenboom, G. Impact of generated solar radiation on simulated crop growth and yield. *Ecol. Model.* **2008**, *210*, 312–326. [CrossRef]

26. Farhadi Bansouleh, B.; Sharifi, M.A.; Van Keulen, H. Sensitivity analysis of performance of crop growth simulation models to daily solar radiation estimation methods in Iran. *Energy Convers. Manag.* **2009**, *50*, 2826–2836. [CrossRef]
27. Allen, R.G.; Walter, I.; Elliott, R.; Howell, T.; Itenfisu, D.; Jensen, M.; Snyder, R. The ASCE Standardized Reference Evapotranspiration Equation. 2005. Available online: https://epic.awi.de/id/eprint/42362/1/ascestzdetmain2005.pdf (accessed on 25 August 2022).
28. Priestley, C.H.B.; Taylor, R.J. On the Assessment of Surface Heat Flux and Evaporation Using Large-Scale Parameters. *Mon. Wea. Rev.* **1972**, *100*, 81–92. [CrossRef]
29. Hargreaves, G.; Samani, Z. Reference crop evapotranspiration from temperature. *Appl. Eng. Agric.* **1985**, *1*, 96. [CrossRef]
30. Trajkovic, S. Temperature-based approaches for estimating reference evapotranspiration. *J. Irrig. Drain. Eng.* **2005**, *131*, 316–323. [CrossRef]
31. Trajkovic, S.; Kolakovic, S. Estimating reference evapotranspiration using limited weather data. *J. Irrig. Drain. Eng.* **2009**, *135*, 443–449. [CrossRef]
32. Todorovic, M.; Karic, B.; Pereira, L.S. Reference evapotranspiration estimate with limited weather data across a range of Mediterranean climates. *J. Hydrol.* **2013**, *481*, 166–176. [CrossRef]
33. Seiller, G.; Anctil, F. How do potential evapotranspiration formulas influence hydrological projections? *Hydrol. Sci. J.* **2016**, *61*, 2249–2266. [CrossRef]
34. Jensen, M.E.; Allen, R.G. Estimates of irrigation water requirements and streamflow depletion. In *Evaporation, Evapotranspiration, and Irrigation Water Requirements*, 2nd ed.; Jensen, M.E., Allen Richard, G., Eds.; ASCE Manuals and Reports on Engineering Practice No. 70; ASCE: New York, NY, USA, 2016; pp. 435–455.
35. Anothai, J.; Soler, C.M.T.; Green, A.; Trout, T.J.; Hoogenboom, G. Evaluation of two evapotranspiration approaches simulated with the CSM–CERES–Maize model under different irrigation strategies and the impact on maize growth, development and soil moisture content for semi-arid conditions. *Agric. For. Meteorol.* **2013**, *176*, 64–76. [CrossRef]
36. Cuadra, S.V.; Kimball, B.A.; Boote, K.J.; Suyker, A.E.; Pickering, N. Energy balance in the DSSAT-CSM-CROPGRO model. *Agric. For. Meteorol.* **2021**, *297*, 108241. [CrossRef]
37. Blaney, H.F.; Criddle, W.D. *Determining Water Requirements in Irrigated Areas from Climatological and Irrigation Data*; SCS-TP 96; U.S. Department Agriculture Soil Conservation Service: Asheville, NC, USA, 1950; p. 44.
38. Makkink, G.F. Testing the Penman formula by means of lysimeters. *J. Inst. Water Eng.* **1957**, *11*, 277–288.
39. Huo, Z.; Dai, X.; Feng, S.; Kang, S.; Huang, G. Effect of climate change on reference evapotranspiration and aridity index in arid region of China. *J. Hydrol.* **2013**, *492*, 24–34. [CrossRef]
40. Nouri, M.; Homaee, M.; Bannayan, M. Quantitative Trend, Sensitivity and Contribution Analyses of Reference Evapotranspiration in some Arid Environments under Climate Change. *Water Resour. Manag.* **2017**, *31*, 2207–2224. [CrossRef]
41. Roderick, M.L.; Rotstayn, L.D.; Farquhar, G.D.; Hobbins, M.T. On the attribution of changing pan evaporation. *Geophys. Res. Lett.* **2007**, *34*, L17403. [CrossRef]
42. Zhang, Y.; Liu, C.; Tang, Y.; Yang, Y. Trends in pan evaporation and reference and actual evapotranspiration across the Tibetan Plateau. *J. Geophys. Res.* **2007**, *112*, D12110. [CrossRef]
43. McVicar, T.R.; Roderick, M.L.; Donohue, R.J.; Li, L.T.; Van Niel, T.G.; Thomas, A.; Grieser, J.; Jhajharia, D.; Himri, Y.; Mahowald, N.M.; et al. Global review and synthesis of trends in observed terrestrial near-surface wind speeds: Implications for evaporation. *J. Hydrol.* **2012**, *416–417*, 182–205. [CrossRef]
44. Araghi, A.; Maghrebi, M.; Olesen, J.E. Effect of wind speed variation on rainfed wheat production evaluated by the CERES-Wheat model. *Int. J. Biometeorol.* **2021**, *66*, 225–233. [CrossRef]
45. Chen, D.; Gao, G.; Xu, C.-Y.; Guo, J.; Ren, G. Comparison of the Thornthwaite method and pan data with the standard Penman-Monteith estimates of reference evapotranspiration in China. *Clim. Res.* **2005**, *28*, 123–132. [CrossRef]
46. Nouri, M.; Homaee, M. On modeling reference crop evapotranspiration under lack of reliable data over Iran. *J. Hydrol.* **2018**, *566*, 705–718. [CrossRef]
47. Razzaghi, F.; Plauborg, F.; Jacobsen, S.-E.; Jensen, C.R.; Andersen, M.N. Effect of nitrogen and water availability of three soil types on yield, radiation use efficiency and evapotranspiration in field-grown quinoa. *Agric. Water Manag.* **2012**, *109*, 20–29. [CrossRef]
48. Di Paolo, E.; Rinaldi, M. Yield response of corn to irrigation and nitrogen fertilization in a Mediterranean environment. *Field Crop. Res.* **2008**, *105*, 202–210. [CrossRef]
49. Doorenbos, J.; Kassam, A. *Yield Response to Water*; Paper 33; FAO Irrigation and Drainage Paper; FAO: Rome, Italy, 1979; p. 193.
50. UNEP. *World Atlas of Desertification*; Arnold, Hodder Headline, PLC: London, UK, 1997; p. 182.
51. Nouri, M.; Homaee, M. Drought trend, frequency and extremity across a wide range of climates over Iran. *Meteorol. Appl.* **2020**, *27*, e1899. [CrossRef]
52. Nouri, M.; Homaee, M. Contribution of soil moisture variations to high temperatures over different climatic regimes. *Soil Tillage Res.* **2021**, *213*, 105115. [CrossRef]
53. Bannayan, M.; Asadi, S.; Nouri, M.; Yaghoubi, F. Time trend analysis of some agroclimatic variables during the last half century over Iran. *Theor. Appl. Climatol.* **2020**, *140*, 839–857. [CrossRef]
54. Saxton, K.E.; Rawls, W.J.; Romberger, J.S.; Papendick, R.I. Estimating Generalized Soil-water Characteristics from Texture. *Soil Sci. Soc. Am. J.* **1986**, *50*, 1031–1036. [CrossRef]
55. Rawls, W.J.; Brakensiek, D.L.; Saxtonn, K.E. Estimation of Soil Water Properties. *Trans. ASAE* **1982**, *25*, 1316. [CrossRef]

56. Nouri, M.; Homaee, M.; Bannayan, M.; Hoogenboom, G. Towards modeling soil texture-specific sensitivity of wheat yield and water balance to climatic changes. *Agric. Water Manag.* **2016**, *177*, 248–263. [CrossRef]
57. Hoogenboom, G.; Porter, C.H.; Boote, K.J.; Shelia, V.; Wilkens, P.W.; Singh, U.; White, J.W.; Asseng, S.; Lizaso, J.I.; Moreno, L.P.; et al. The DSSAT crop modeling ecosystem. In *Advances in Crop Modelling for a Sustainable Agriculture*; Boote, K., Ed.; Burleigh Dodds Science Publishing: Cambridge, UK, 2019; pp. 173–216.
58. Hoogenboom, G.; Porter, C.H.; Shelia, V.; Boote, K.J.; Singh, U.; White, J.W.; Hunt, L.A.; Ogoshi, R.; Lizaso, J.I.; Koo, J.; et al. *Decision Support System for Agrotechnology Transfer (DSSAT)*; Version 4.7.5; DSSAT Foundation: Gainesville, FL, USA, 2019; Available online: https://DSSAT.net (accessed on 1 June 2020).
59. Saseendran, S.A.; Ahuja, L.R.; Ma, L.; Timlin, D.; Stöckle, C.O.; Boote, K.J.; Hoogenboom, G. Current water deficit stress simulations in selected agricultural system models. In *Response of Crops to Limited Water: Understanding and Modeling Water Stress Effects on Plant Growth Processes*; Ahuja, L.R., Reddy, V.R., Saseendran, S.A., Yu, Q., Eds.; American Society of Agronomy, Inc., Crop Science Society of America, Inc., Soil Science Society of America, Inc.: Madison, WI, USA, 2008; Volume 1, pp. 1–38.
60. Hanks, R.J. Model for predicting plant yield as influenced by water use. *Agron. J.* **1974**, *66*, 660–665. [CrossRef]
61. de Wit, C.T. *Transpiration and Crop Yields*; Institute of Biological and Chemical Research on Field Crops and Herbage: Wageningen, The Netherlands, 1958; p. 88.
62. Paredes, P.; Rodrigues, G.C.; Alves, I.; Pereira, L.S. Partitioning evapotranspiration, yield prediction and economic returns of maize under various irrigation management strategies. *Agric. Water Manag.* **2014**, *135*, 27–39. [CrossRef]
63. Suleiman, A.A.; Ritchie, J.T. Modifications to the DSSAT vertical drainage model for more accurate soil water dynamics estimation. *Soil Sci.* **2004**, *169*, 745–757. [CrossRef]
64. Ritchie, J.T.; Porter, C.H.; Judge, J.; Jones, J.W.; Suleiman, A.A. Extension of an Existing Model for Soil Water Evaporation and Redistribution under High Water Content Conditions. *Soil Sci. Soc. Am. J.* **2009**, *73*, 792–801. [CrossRef]
65. Ritchie, J.T. Water dynamics in the soil-plant-atmosphere system. *Plant Soil* **1981**, *58*, 81–96. [CrossRef]
66. Ritchie, J.T. Soil water balance and plant water stress. In *Understanding Options for Agricultural Production. Systems Approaches for Sustainable Agricultural Development*; Tsuji, G., Hoogenboom, G., Thornton, P., Eds.; Springer: Dordrecht, The Netherlands, 1998; pp. 41–54.
67. Williams, J.R.; Jones, C.A.; Dyke, P.T. A modeling approach to determining the relationship between erosion and soil productivity. *Trans. ASAE* **1984**, *27*, 129–144. [CrossRef]
68. Cristea, N.C.; Kampf, S.K.; Burges, S.J. Revised Coefficients for Priestley-Taylor and Makkink-Hansen Equations for Estimating Daily Reference Evapotranspiration. *J. Hydrol. Eng.* **2013**, *18*, 1289–1300. [CrossRef]
69. Martínez-Cob, A.; Tejero-Juste, M. A wind-based qualitative calibration of the Hargreaves ET_0 estimation equation in semiarid regions. *Agric. Water Manag.* **2004**, *64*, 251–264. [CrossRef]
70. Tabari, H.; Talaee, P.H. Local Calibration of the Hargreaves and Priestley-Taylor Equations for Estimating Reference Evapotranspiration in Arid and Cold Climates of Iran Based on the Penman-Monteith Model. *J. Hydrol. Eng.* **2011**, *16*, 837–845. [CrossRef]
71. Moratiel, R.; Bravo, R.; Saa, A.; Tarquis, A.M.; Almorox, J. Estimation of evapotranspiration by the Food and Agricultural Organization of the United Nations (FAO) Penman–Monteith temperature (PMT) and Hargreaves–Samani (HS) models under temporal and spatial criteria—A case study in Duero basin (Spain). *Nat. Hazards Earth Syst. Sci.* **2020**, *20*, 859–875. [CrossRef]
72. Liu, J.; Williams, J.R.; Wang, X.; Yang, H. Using MODAWEC to generate daily weather data for the EPIC model. *Environ. Model.* **2009**, *24*, 655–664. [CrossRef]
73. Meyer, W.S. *Standard Reference Evaporation Calculation for Inland, South Eastern Australia*; Laboratory Technical Report 35/98; CSIRO Land and Water: Adelaide, Australia, 1999; p. 30.
74. Doorenbos, J.; Pruitt, W.O. *Guidelines for Predicting Crop Water Requirements*; FAO Irrigation and Drainge Papers, No. 24; Food and Agricultural Organization of the United Nations: Rome, Italy, 1977; p. 154.
75. Droogers, P.; Allen, R.G. Estimating Reference Evapotranspiration Under Inaccurate Data Conditions. *Irrig. Drain. Syst.* **2002**, *16*, 33–45. [CrossRef]
76. Ravazzani, G.; Corbari, C.; Morella, S.; Gianoli, P.; Mancini, M. Modified Hargreaves-Samani equation for the assessment of reference evapotranspiration in Alpine river basins. *J. Irrig. Drain. Eng.* **2012**, *138*, 592–599. [CrossRef]
77. Paredes, P.; Pereira, L.S.; Almorox, J.; Darouich, H. Reference grass evapotranspiration with reduced data sets: Parameterization of the FAO Penman-Monteith temperature approach and the Hargeaves-Samani equation using local climatic variables. *Agric. Water Manag.* **2020**, *240*, 106210. [CrossRef]
78. Nouri, M.; Ebrahimipak, N.A.; Hosseini, S.N. Estimating reference evapotranspiration for water-limited windy areas under data scarcity. *Theor. Appl. Climatol.* **2022**, *150*, 593–611. [CrossRef]
79. Paredes, P.; Fontes, J.C.; Azevedo, E.B.; Pereira, L.S. Daily reference crop evapotranspiration with reduced data sets in the humid environments of Azores islands using estimates of actual vapor pressure, solar radiation, and wind speed. *Theor. Appl. Climatol.* **2017**, *134*, 1115–1133. [CrossRef]
80. Trajkovic, S.; Gocic, M. Evaluation of three wind speed approaches in temperature-based ET0 equations: A case study in Serbia. *Arab. J. Geosci.* **2021**, *14*, 35. [CrossRef]
81. Dettori, M.; Cesaraccio, C.; Motroni, A.; Spano, D.; Duce, P. Using CERES-Wheat to simulate durum wheat production and phenology in Southern Sardinia, Italy. *Field Crop. Res.* **2011**, *120*, 179–188. [CrossRef]

82. Gereña, A.; Ruiz-Ramos, M.; Díaz-Ambrona, C.H.; Conde, J.R.; Mínguez, M.I. Assessment of climate change and agriculture in Spain using climate models. *Agron. J.* **2001**, *93*, 237–249. [CrossRef]
83. Xiong, W.; Lin, E.; Ju, H.; Xu, Y.J.C.C. Climate change and critical thresholds in China's food security. *Clim. Change* **2007**, *81*, 205–221. [CrossRef]
84. Tao, F.; Zhang, Z. Impacts of climate change as a function of global mean temperature: Maize productivity and water use in China. *Clim. Change* **2011**, *105*, 409–432. [CrossRef]
85. Wang, W.; Xing, W.; Shao, Q. How large are uncertainties in future projection of reference evapotranspiration through different approaches? *J. Hydrol.* **2015**, *524*, 696–700. [CrossRef]
86. Wang, W.; Li, C.; Xing, W.; Fu, J. Projecting the potential evapotranspiration by coupling different formulations and input data reliabilities: The possible uncertainty source for climate change impacts on hydrological regime. *J. Hydrol.* **2017**, *555*, 298–313. [CrossRef]
87. Randall, D.A.; Wood, R.A.; Bony, S.; Colman, R.; Fichefet, T.; Fyfe, J.; Kattsov, V.; Pitman, A.; Shukla, J.; Srinivasan, J. Climate models and their evaluation. In *Climate Change 2007: The Physical Science Basis*; Contribution of Working Group I to the Fourth Assessment Report of the IPCC (FAR); Solomon, S., Randall, D.A., Wood, R.A., Bony, S., Colman, R., Fichefet, T., Fyfe, J., Kattsov, V., Pitman, A., Shukla, J., et al., Eds.; Cambridge University Press: Cambridge, UK, 2007; pp. 589–662.